Article

Arabidopsis TANGLED Identifies the Division Plane throughout Mitosis and Cytokinesis

Keely L. Walker,[1,3] Sabine Müller,[1,2,4] Dorianne Moss,[2] David W. Ehrhardt,[2] and Laurie G. Smith[1,*]

[1]Section of Cell and Developmental Biology
University of California, San Diego
9500 Gilman Drive
La Jolla, California 92093-0116
[2]Carnegie Institution
Department of Plant Biology
260 Panama Street
Stanford, California 94305

Summary

Background: In premitotic plant cells, the future division plane is predicted by a cortical ring of microtubules and F-actin called the preprophase band (PPB). The PPB persists throughout prophase, but is disassembled upon nuclear-envelope breakdown as the mitotic spindle forms. Following nuclear division, a cytokinetic phragmoplast forms between the daughter nuclei and expands laterally to attach the new cell wall at the former PPB site. A variety of observations suggest that expanding phragmoplasts are actively guided to the former PPB site, but little is known about how plant cells "remember" this site after PPB disassembly.
Results: In premitotic plant cells, *Arabidopsis* TANGLED fused to YFP (AtTAN::YFP) colocalizes at the future division plane with PPBs. Strikingly, cortical AtTAN::YFP rings persist after PPB disassembly, marking the division plane throughout mitosis and cytokinesis. The AtTAN::YFP ring is relatively broad during preprophase/prophase and mitosis; narrows to become a sharper, more punctate ring during cytokinesis; and then rapidly disassembles upon completion of cytokinesis. The initial recruitment of AtTAN::YFP to the division plane requires microtubules and the kinesins POK1 and POK2, but subsequent maintenance of AtTAN::YFP rings appears to be microtubule independent. Consistent with the localization data, analysis of *Arabidopsis tan* mutants shows that AtTAN plays a role in guidance of expanding phragmoplasts to the former PPB site.
Conclusions: AtTAN is implicated as a component of a cortical guidance cue that remains behind when the PPB is disassembled and directs the expanding phragmoplast to the former PPB site during cytokinesis.

Introduction

In plants, where cells are embedded in a matrix of wall material and do not migrate, relative cell positions

*Correspondence: lgsmith@ucsd.edu
[3]Present address: Office of Faculty and Institutional Support, City of Hope, 1500 E. Duarte Road, Duarte California 91010.
[4]Present address: School of Biological Sciences, The University of Auckland, Private Bag 92019, Auckland Mail Centre, Auckland 1142, New Zealand.

are permanently established when daughter cells are formed at cytokinesis. Consequently, proper orientation of division planes during development is critical for the cellular organization of plant tissues. Unlike most other eukaryotic cells, the division planes of plant cells are established prior to mitosis. During S or G_2 phase of the cell cycle, most plant cells form a cortical ring of microtubules and F-actin called the preprophase band (PPB) at the future division plane as the premitotic nucleus migrates into this plane [1]. The PPB persists throughout prophase, but is disassembled upon nuclear-envelope breakdown as the mitotic spindle forms [1, 2]. During cytokinesis, a new cell wall (cell plate) is initiated through the action of the phragmoplast, another F-actin- and microtubule-based structure. The disk-shaped phragmoplast is assembled between daughter nuclei and expands laterally to complete cytokinesis, guiding cell-plate attachment at the site formerly occupied by the PPB [3, 4].

The observation that PPBs accurately predict the future division plane in a wide variety of plant cell types strongly suggests that the PPB plays a key role in division-plane establishment [1, 5]. Further supporting this idea, genetic [6] or pharmacological [7] disruption of PPBs causes cells to divide in aberrant orientations. A variety of observations have indicated that some type of cue is present at the former location of the PPB and functions to guide phragmoplast expansion to this site [8]. For example, if a spindle is mechanically displaced from the plane defined by the former PPB, phragmoplasts often migrate back to the former PPB site as they expand [9, 10]. Furthermore, in some cell types, spindles normally rotate to an oblique orientation during mitosis. When this occurs, the phragmoplast is initially oriented obliquely, but rotates as cytokinesis proceeds so that the cell plate attaches at the former PPB site [11, 12]. Thus, the PPB has long been thought to function during prophase to establish a "cortical division site" that guides the expanding phragmoplast during cytokinesis [5, 8, 13].

Identification of the molecular features of the cortical division site has been a longstanding challenge. During mitosis and cytokinesis, the former PPB site is "negatively marked" by local depletion of cortical F-actin [14–16] and a kinesin, KCA1 [7]. The depletion of these two proteins has been proposed to play an important role in the maintenance or function of the cortical division site. A novel microtubule-associated protein, AIR9, colocalizes with PPBs but disappears from the cortex upon PPB disassembly, later reappearing at the cortical division site when the cell plate inserts there [17]. Similarly, two other proteins are localized at the cortical division site or adjacent cell wall just as the cell plate attaches there: RSH, a hydroxyproline-rich glycoprotein [18], and T-PLATE, a protein with domains similar to those of vesicular-coat proteins [19]. Thus, AIR9, RSH, and T-PLATE are all implicated in cell-plate attachment at the cortical division site and/or cell-plate maturation.

However, proteins that are recruited to the division site by the PPB and remain localized there after PPB disassembly have not been identified.

Previous studies established that the *tangled* (*tan*) gene plays an important role in the spatial control of cytokinesis in maize [20]. In *tan* mutants, cells in all tissues divide in aberrant orientations because of the frequent failure of phragmoplasts to be guided to former PPB sites [12]. The highly basic maize TAN protein binds to microtubules in vitro, but is not closely related to other proteins of known function [21]. Proteins recognized by anti-TAN antibodies were shown by immunofluorescence microscopy to associate with PPBs, spindles, and phragmoplasts in dividing cells and to be present in the cytoplasm throughout the cell cycle [21]. However, these antibodies were not completely specific for TAN [21]; they apparently also recognized TAN-related proteins that are likely to be the products of expressed, *tan*-related genes that were recently identified via EST sequencing (e.g., TIGR Gene Indexes TC311793, TC290411, DR791368). Therefore, the intracellular localization of maize TAN has not been definitively determined.

To advance our understanding of TAN localization and function, we investigated the *Arabidopsis* TANGLED homolog (AtTAN). Here we show that AtTAN::YFP is recruited in a microtubule- and kinesin-dependent manner to the cortical division site, where it colocalizes with PPBs and persists at the division site after PPB disassembly, positively marking this site throughout the remainder of the cell cycle. We also present genetic evidence that AtTAN plays a role in phragmoplast guidance. Thus, AtTAN is implicated as a component of a cortical cue that preserves the memory of the PPB throughout mitosis and cytokinesis.

Results

Arabidopsis TANGLED::YFP Localizes as a Ring at the Cortical Division Site throughout Mitosis and Cytokinesis

A BLAST search of the *Arabidopsis* genome revealed a single gene that encodes a protein significantly similar to maize TAN. The full-length coding sequence of *Arabidopsis TAN* (*AtTAN*; At3g05330) was determined by sequencing of a cDNA clone and RT-PCR products. Like maize TAN (pI 12.6), AtTAN is highly basic, with a pI of 12.3. AtTAN (53 kD) is 29% larger than maize TAN (41 kD), mainly because of internal sequence duplications that are near the carboxyl terminus of the *Arabidopsis* protein and are not found in maize TAN or its other dicot homologs (Figure S1 in the Supplemental Data available online). AtTAN is 35% identical overall to maize TAN; its amino-terminal half (245 amino acids) is 48% identical to the corresponding region of maize TAN (Figure S1). Analysis of an *AtTAN* promoter::β-glucuronidase reporter together with northern-blot analysis demonstrated that *AtTAN* expression correlates with cell division (Figure S2), as previously shown for maize *tan* [21].

To investigate the localization of AtTAN protein, we fused yellow fluorescent protein (YFP) to its carboxyl terminus and expressed the fusion protein from either the native promoter or a constitutive CaMV 35S promoter in transgenic plants. In both cases, AtTAN::YFP
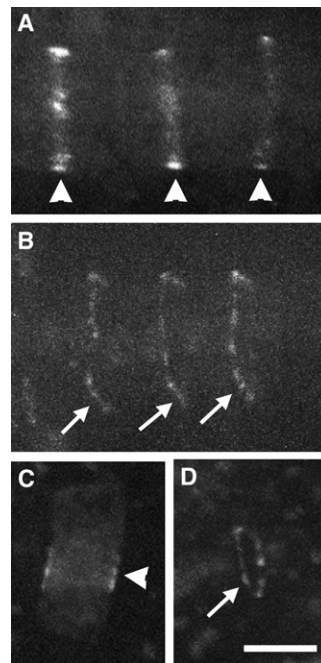

Figure 1. *Arabidopsis* and Maize TAN Fluorescent Fusion Proteins Form Rings in a Subset of Root-Tip Cells in Transgenic *Arabidopsis*

Arrowheads point to broad, diffuse rings found in cells with a single nucleus, and arrows point to sharper, denser, more punctate rings found in cells with divided nuclei.
(A and B) Localization of *Arabidopsis* TAN::YFP expressed from its native promoter (1.34 kb of genomic sequence upstream of the ATG).
(C and D) Localization of maize TAN::GFP expressed from the CaMV 35S promoter. The scale bar represents 10 μm.

localized in well-defined, peripheral rings found in a subset of root-tip cells. Two distinct classes of rings were observed: broad, diffuse rings (Figure 1A), and sharper, denser rings (Figure 1B). When expressed from the CaMV 35S promoter in transgenic *Arabidopsis*, maize TAN fused at its carboxyl terminus to GFP localized similarly, also forming either broad (Figure 1C) or sharp (Figure 1D) rings in a subset of root-tip cells.

To clarify how AtTAN::YFP rings relate to mitotic microtubule arrays, we transformed plants expressing AtTAN::YFP with a 35S promoter::CFP::α-tubulin (CFP::TUA1) construct [22]. In root tip cells with PPBs, AtTAN::YFP formed a diffuse ring that colocalized precisely with the PPB (n > 60; Figures 2A–2D). In cells with mitotic spindles, AtTAN::YFP was localized at the future division plane as a diffuse ring of the same width as a PPB-associated ring (n > 35; Figure 2E–2H). In cells with phragmoplasts, AtTAN::YFP rings were sharper and denser than those in cells with PPBs or spindles, and they precisely circumscribed the midplane of the phragmoplast (n > 100; Figures 2I–2P). These sharp rings were relatively continuous in cells at early stages of cytokinesis (Figures 2I–2L), but appeared distinctly punctate at later stages (Figures 2M–2P). Analysis of AtTAN::YFP and CFP::TUA1 was focused mainly on root tips, where most cell divisions are transverse to the long axis of the root, but we observed similar results in tissues where other patterns of division occur, such as newly emerged cotyledons and leaf primordia.
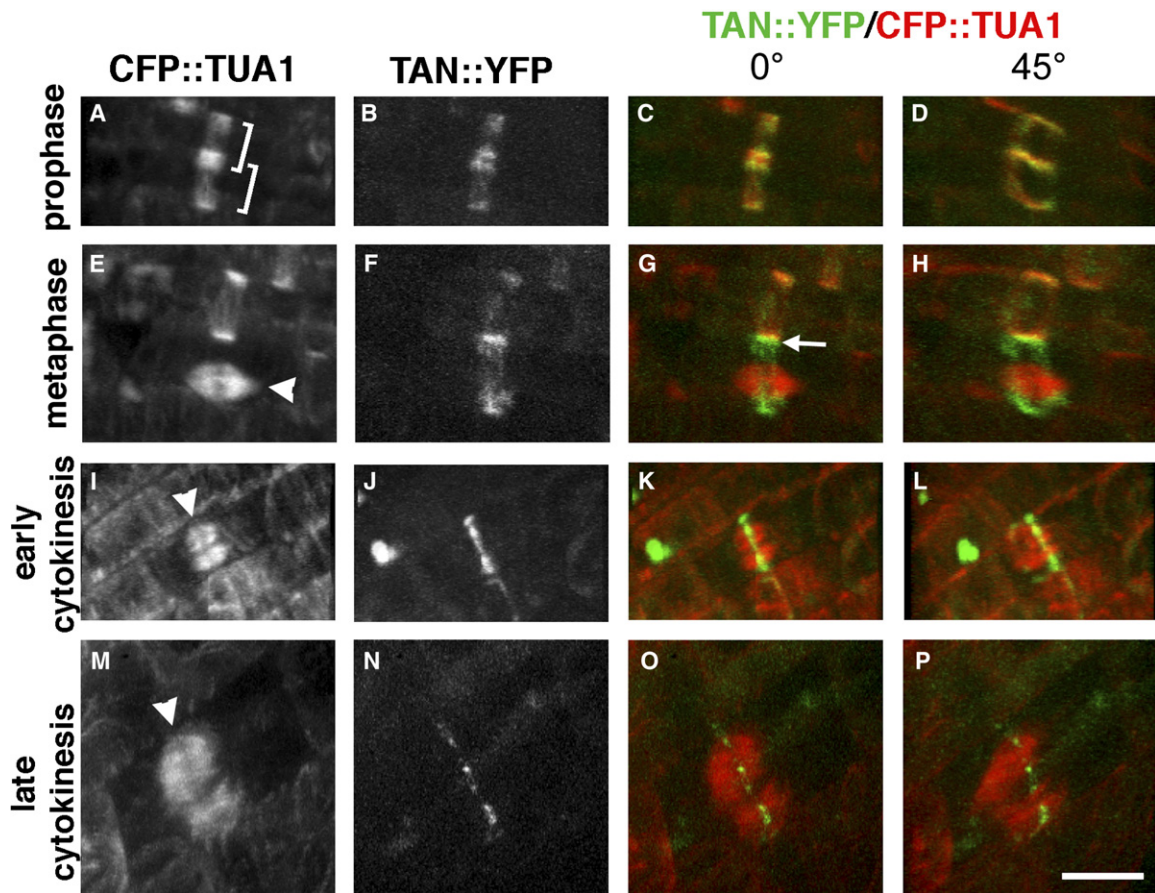
Figure 2. *Arabidopsis* TAN::YFP Localizes as a Ring at the Division Site throughout Mitosis and Cytokinesis in Root-Tip Cells

(A–P) Dual localization of 35S-AtTAN::YFP (monochrome in second column, green in third and fourth column) and 35S-CFP::TUA1 (monochrome in first column, red in third and fourth columns) in cells at the indicated cell-cycle stages. Brackets in (A) indicate a pair of adjacent PPBs. Arrowheads point to a metaphase spindle in (E) and to phragmoplasts in (I) and (M). The arrow in (G) points to the junction between a spindle-associated AtTAN::YFP ring and the adjacent PPB. In (D), (H), and (L), 45° rotations show that AtTAN::YFP forms a complete ring encircling the cell. The scale bar represents 10 μm.

Time-lapse observations were made to investigate the timing of changes in AtTAN::YFP localization in single cells as they progress through the cell cycle. As illustrated in Figures 3A–3E for the cell shown at time zero (metaphase) in Figures 2E–2H, broad AtTAN::YFP rings began to narrow as soon as a phragmoplast was initiated (Figure 3C) and sharpened further during the course of phragmoplast expansion to the cell periphery (n = 5; Figures 3D and 3E). Time-lapse imaging of cells at later stages of cytokinesis, when phragmoplasts had already expanded to the cell periphery, showed that AtTAN::YFP rings persisted through the completion of cell-plate insertion and then disintegrated (n = 11). For example, in the cell shown in Figures 3F–3I, an expanded phragmoplast initially appeared in an arc across the upper half of the cell, having previously reached the plasma membrane and disassembled in the lower half of the cell; the punctate AtTAN::YFP ring was clearly visible as bright spots around the entire cell equator (Figure 3F). As cytokinesis proceeded (Figures 3G–3I), disintegration of AtTAN::YFP puncta followed disassembly of the phragmoplast from the corresponding position at the cell periphery by 10–20 min. Low levels of 35S-promoter-driven AtTAN::YFP were observed in

the cytoplasm of interphase cells, but native promoter-driven AtTAN::YFP was only detectable in cells with cortical rings (data not shown), suggesting cell-cycle-regulated accumulation of TAN protein and/or *TAN* mRNA.

In summary, AtTAN::YFP forms cortical rings that, together with PPBs, demarcate the future division plane in premitotic cells. Unlike PPBs, however, AtTAN::YFP rings persist at the cortical division site throughout mitosis. The initially broad AtTAN::YFP rings seen in cells with PPBs and spindles narrow down during cytokinesis to become sharper, more punctate rings, which disintegrate shortly after cell-plate insertion.

Initial Recruitment of *Arabidopsis* TAN::YFP to the Division Site Requires Microtubules

To investigate the role of the PPB in AtTAN::YFP localization at the division site, we carried out inhibitor studies to determine whether AtTAN::YFP localization requires microtubules. Five micromolar oryzalin, a microtubule-destabilizing drug, was applied to cells that had formed PPBs, and these cells were subsequently observed at 5 min intervals for 10–20 min. As shown in Figure 4A, the addition of 5 μM oryzalin caused disassembly of the PPB microtubules within 5 min of drug
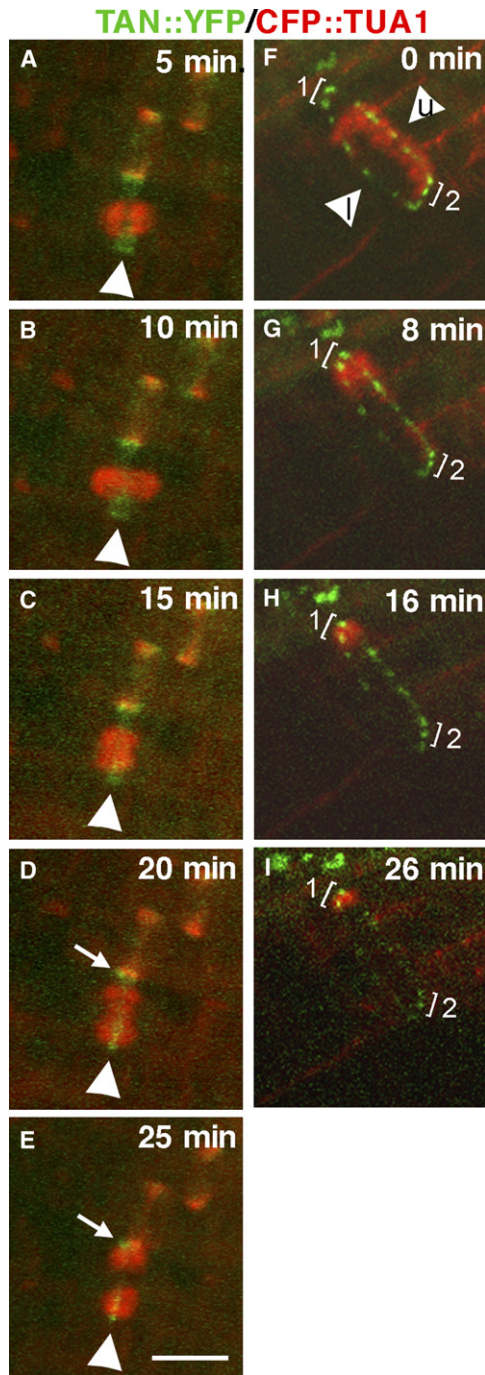
Figure 3. Time-Lapse Analysis of Changes in the Appearance of AtTAN::YFP Rings during Cell Division

In all panels, AtTAN::YFP is shown in green and CFP::TUA1 in red. (A–E) The metaphase cell shown at time zero in Figures 2E–2H was subsequently imaged every 5 min as indicated. Arrowheads point to an AtTAN::YFP ring in a cell with a metaphase spindle (A), an elongated spindle (B), a newly initiated phragmoplast (C), an expanded phragmoplast (D), and a more expanded phragmoplast (E). Arrows in (D) and (E) point to the edge of a broad, PPB-associated AtTAN::YFP ring in the adjacent cell.

(F–I) A cell completing cytokinesis was imaged every 8–10 min as indicated. In (F), a highly punctate, but complete, AtTAN::YFP ring encircles a cell with a phragmoplast that has expanded to the upper face of the cell (arrowhead marked "u") and has already disassembled at the lower face (arrowhead marked "l"; note that

addition, but failed to alter AtTAN::YFP localization during the observation period (n = 13). Therefore, short-term maintenance of broad AtTAN::YFP rings that have already formed appears to be largely microtubule independent.

Further experiments were conducted to determine whether the initial recruitment of AtTAN::YFP to the division site requires microtubules. Seedlings were mounted on coverslips in the presence or absence of 5 μM oryzalin. Root tips were examined immediately, and again 120 min later, for the presence of AtTAN::YFP rings. Time-zero and 120 min images of the same root tips were directly compared to distinguish new rings (those present at 120 min but absent at time zero) from older rings. In the absence of oryzalin, 16 of 24 broad rings present at 120 min were new (Table 1). Consistent with our earlier finding that AtTAN::YFP rings sharpen late in the cell cycle and disintegrate shortly after completion of cytokinesis, no sharp rings present at time zero remained after 120 min in the absence of oryzalin: 12 of 16 were new (Table 1), and the remaining 4 arose from rings that were broad at time zero. Extending the results of the short-term oryzalin-treatment experiments described earlier, 11 of 25 broad rings present at time zero were still present after 120 min in oryzalin (e.g., single arrowhead, Figure 4B), but no new broad rings formed in the presence of oryzalin (Table 1). As in control roots, all sharp rings present at time zero disappeared during 120 min of oryzalin treatment, and no new sharp rings formed (Table 1). Thus, new AtTAN::YFP rings consistently formed in the absence but not in the presence of oryzalin, suggesting that microtubules are required for the initial recruitment of AtTAN::YFP to the division site.

Additional experiments were carried out to investigate whether the lack of AtTAN::YFP ring formation in the presence of oryzalin could be due simply to inhibition of cell-cycle initiation by oryzalin. Seedlings were treated as before for 2 hr with or without 5 μM oryzalin, then fixed and stained for nucleic acids to identify cells with condensed chromosomes, indicating that they were in mitosis (Figure S3). The frequency of cells with condensed chromosomes was higher in oryzalin-treated roots (13.4/root, n = 10 roots) than in control roots (3.6/root, n = 10 roots), as expected if cells continue to enter the cell cycle during the oryzalin treatment, but are unable to progress through mitosis because of lack of microtubule function. Indeed, microtubule-depolymerizing drugs are commonly used as a tool to increase the frequency of mitotic cells because of their ability to block the cell cycle at prometaphase (e.g., [23]). Thus, the failure of AtTAN::YFP rings to form in oryzalin does not appear to be due to inhibition of cell-cycle initiation by the drug treatment, supporting the conclusion that initial recruitment of AtTAN::YFP to the division plane is microtubule dependent. However,

---

AtTAN::YFP puncta in bracketed areas 1 and 2 are equally bright at time zero). Subsequently, the phragmoplast completes its expansion into the corner marked by bracket 1 while disassembling elsewhere. By 8 min (G), the AtTAN::YFP ring has already begun to disintegrate at the lower face of the cell, and by 26 min (I), it has also disintegrated at the upper face and at the area marked by bracket 2 while persisting at the corner marked with bracket 1, where the phragmoplast has not yet disassembled. The scale bar represents 10 μm.
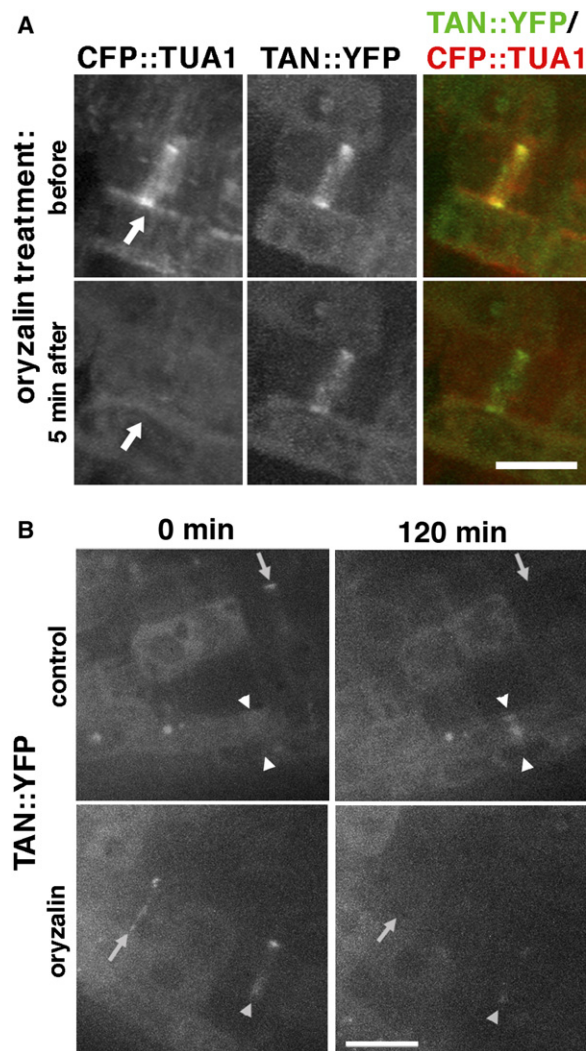
Figure 4. Analysis of the Role of Microtubules in AtTAN::YFP Recruitment and Retention at the Division Site

All images shown are Z projections of confocal stacks.
(A) CFP::TUA1 (monochrome in first column, red in third column) and AtTAN::YFP (monochrome in second column, green in third column) in a cell with a PPB (arrows) before (top) and 5 min after (bottom) perfusion of 5 μM oryzalin under the coverslip. The AtTAN::YFP ring persists after disassembly of PPB microtubules.
(B) AtTAN::YFP rings (monochrome only) observed in root tips treated with 5 μM oryzalin (bottom) or no oryzalin (top). Root tips were examined at 0 min (left) and again at 120 min (right). Comparison of 0 min and 120 min images for the same roots revealed rings that disappeared (arrows) or faded (single arrowhead) during the observation period in the presence or absence of oryzalin, but new rings (i.e., absent at 0 min but present at 120 min; double arrowheads) formed only in the absence of oryzalin. The scale bar represents 10 μm.

inhibition of cell-cycle progression through metaphase by oryzalin precludes any conclusions from these experiments regarding the possible role of microtubules in maintaining existing AtTAN::YFP rings after prophase or in sharpening of AtTAN::YFP rings during cytokinesis.

Taking a complementary approach to further investigate the role of PPB microtubules in recruitment of AtTAN to the division plane, we also expressed AtTAN::YFP and CFP::TUA1 in *tonneau 2* (*ton2*) mutants, which

Table 1. Summary of Results for All AtTAN::YFP Rings Observed in Ten Roots of Each Genotype Treated and Analyzed as Described in the Legend to Figure 4B

	0 min	120 min	New
Control			
broad	32	24[b]	16[a]
sharp	39	16[a]	12[a]
total	71	40[a]	28[a]
Oryzalin			
broad	25	11[b]	0[a]
sharp	38	0[a]	0[a]
total	63	11[a]	0[a]

Broad rings are like those seen in cells with PPBs and spindles (e.g., Figures 2B–2D and 2F–2H); sharp rings are like those seen in cells with phragmoplasts (e.g., Figures 2J–2L and 2N–2P). Pairs of corresponding control versus oryzalin values that are significantly different at $p < 0.001$ or $p < 0.05$ (determined via Mann-Whitney U test analysis of results for individual roots, which were combined to obtain the cumulative values shown in the table) are marked with [a] or [b].
[a] $p < 0.001$.
[b] $p < 0.05$.

fail to form PPBs but do form spindles and phragmoplasts [6, 24]. AtTAN::YFP rings were observed in 12/12 cells with spindles and 10/13 cells with phragmoplasts in YFP+ wild-type siblings of *ton2* mutants, but were not observed in YFP+ *ton2* mutant cells with phragmoplasts (n = 10) or spindles (n = 9; Figure 5A).

In summary, a combination of pharmacological and genetic experiments strongly supports the conclusion that the initial recruitment of AtTAN::YFP to the cortical division site depends on microtubules, but that microtubules are not required for subsequent retention of broad AtTAN::YFP rings at the cortex once they have formed.

Localization of *Arabidopsis* TAN::YFP to the Division Site Requires the Kinesins POK1 and POK2
We previously described a pair of closely related *Arabidopsis* kinesins that are required for the spatial control of cytokinesis, POK1 and POK2 [25]. Similar to *tan* mutants of maize, a high proportion of *pok1;2* double-mutant phragmoplasts fail to be guided to former PPB sites [25]. The COOH terminus of POK1 interacts with AtTAN in the yeast two-hybrid system, suggesting that POK1 might interact directly with AtTAN in vivo [25]. To test the hypothesis that these kinesins function in the localization of AtTAN to the division plane, we introduced AtTAN::YFP and CFP::TUA1 into *pok1;2* double mutants. In nine of 11 YFP+ *pok1;2* mutant cells with PPBs, AtTAN::YFP rings were either faint or absent (Figure 5B), whereas the remaining two had well-defined AtTAN::YFP rings. None of the 29 YFP+ *pok1;2* mutant cells observed with spindles (n = 12) or phragmoplasts (n = 17) had well-defined AtTAN::YFP rings, although faint, diffuse AtTAN::YFP accumulations were sometimes observed (Figure 5C). By contrast, all cells with PPBs (n = 11; Figure 5B), spindles (n = 12), and phragmoplasts (n = 11) in YFP+ wild-type siblings of *pok1;2* mutants had well-defined AtTAN::YFP rings. Therefore, POK1 and POK2 in combination are required for efficient localization of AtTAN::YFP at the division site.
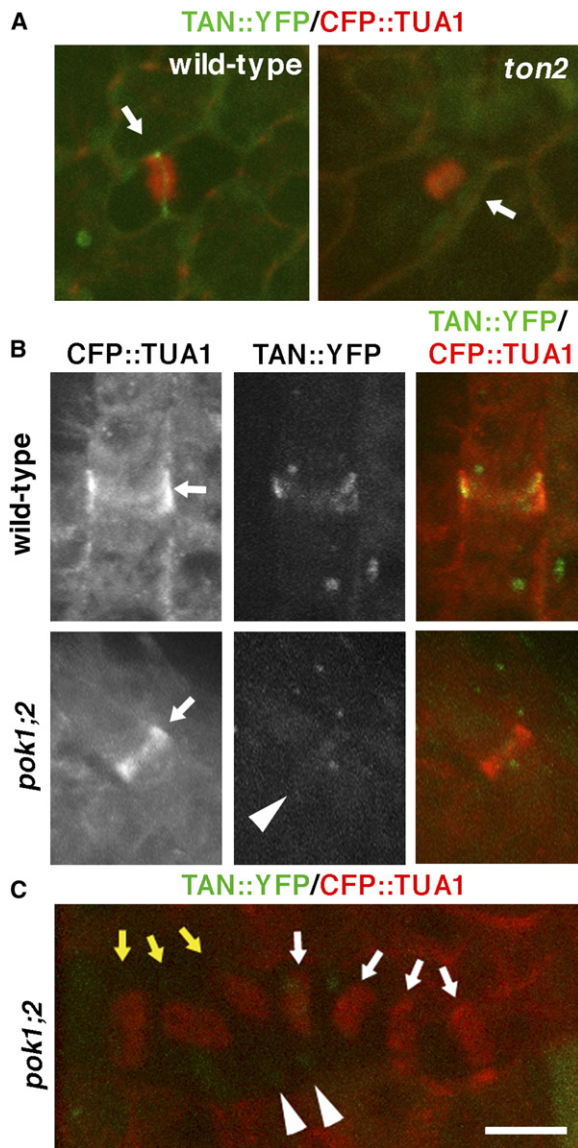
Figure 5. TON2 and POK1/POK2 Are Required for Localization of AtTAN::YFP at the Division Site

(A) Arrows point to cells with phragmoplasts in plants expressing AtTAN::YFP (green) and CFP::TUA1 (red) that are wild-type (left) or *ton2* mutant (right). The wild-type cell has a well-defined AtTAN::YFP ring, and the *ton2* mutant cell does not.

(B) Arrows point to a PPB in a wild-type plant (top) and a *pok1;2* double-mutant plant (bottom) expressing AtTAN::YFP (monochrome in second column, green in third column) and CFP::TUA1 (monochrome in first column, red in third column). The wild-type cell has a well-defined AtTAN::YFP ring, whereas the *pok1;2* double-mutant cell has only a very faint accumulation of AtTAN::YFP (arrowhead).

(C) *pok1;2* double-mutant cells with spindles (yellow arrows) and phragmoplasts (white arrows) labeled with CFP::TUA1 (red) lack well-defined AtTAN::YFP rings (green). Arrowheads point to faint local accumulations of AtTAN::YFP (compare to wild-type AtTAN::YFP ring in [A]). The scale bar represents 10 μm.

Arabidopsis TANGLED Plays a Role in Phragmoplast Guidance in Dividing Root-Tip Cells

Maize TAN is required for guidance of phragmoplasts to former PPB sites [12]. Phenotypes resulting from mutations in the *Arabidopsis TAN* gene were examined to determine whether AtTAN also has this function. Plants homozygous for each of three *tan* alleles with insertions near the beginning of the gene (*tan-csh*, *tan-mad*, and *tan-riken*; see Supplemental Data for additional characterization) appeared morphologically normal but exhibited cell-pattern defects in root tips, indicative of aberrantly oriented cell divisions (Figures 6A–6D). Analysis of microtubule arrays in root tips of *tan-csh* mutants revealed a defect in phragmoplast guidance similar to, but weaker than, that observed previously in *tan* mutants of maize [12] and *pok1;2* double mutants of *Arabidopsis* [25]. In both wild-type and *tan-csh* mutant root-tip cells, 100% of PPBs were oriented transversely or longitudinally to the cell's long axis (wild-type, n = 56; *tan-csh*, n = 51; Figures 6E and 6F). In wild-type root tips, 100% of late phragmoplasts (those spanning the full width of the mother cell) were also oriented within 15° of the transverse or longitudinal cell axis (n = 54; Figure 6G). By contrast, nine of 79 late phragmoplasts observed in *tan-csh* mutant root tips (11%) were tilted ≥ 15° from the transverse or longitudinal axis of the mother cell (Figure 6H). Thus, in *tan-csh* mutant root tips, a significant (p < 0.01 by χ^2 test) proportion of phragmoplasts were not properly guided to former PPB sites, demonstrating that TAN plays a role in phragmoplast guidance in *Arabidopsis* roots. The low frequency of aberrantly oriented divisions observed in *Arabidopsis tan* mutant roots may indicate the existence of a TAN-independent mechanism acting together with TAN to guide phragmoplast expansion in root cells, or may be due to the presence of residual and/or truncated TAN proteins that could potentially accumulate in all three mutants analyzed (see Supplemental Data). The aberrant division pattern observed in *Arabidopsis tan* mutant roots did not alter root growth rate or diameter (Supplemental Data), consistent with earlier findings for maize *tan* mutants where misoriented divisions in leaves have no impact on leaf shape [20].

Discussion

A long-standing hypothesis [5, 8, 13] holds that the PPB functions to direct the assembly of a cortical division site, which preserves the memory of the division plane following PPB disassembly and interacts with the phragmoplast during cytokinesis to guide cell-plate insertion at the former PPB site. Our findings for the localization and function of *Arabidopsis* TANGLED (AtTAN) fulfill several predictions of this hypothesis. Genetic analysis showed, as previously demonstrated for maize TAN, that AtTAN plays a role in guidance of phragmoplasts to former PPB sites in dividing root cells. AtTAN::YFP colocalizes with PPBs in preprophase/prophase cells and remains localized as a cortical ring after PPB disassembly, positively marking the former PPB site throughout mitosis and cytokinesis. Consistent with the hypothesis that the PPB directs the formation of AtTAN::YFP rings, pharmacological and genetic studies showed that the initial recruitment of AtTAN::YFP to the cortical division site requires microtubules and also requires the kinesins POK1 and POK2. Because most kinesins function as microtubule-based motors, these findings suggest that AtTAN may be a cargo for POK1/2, and that POK1/2 function may be at least partly responsible for
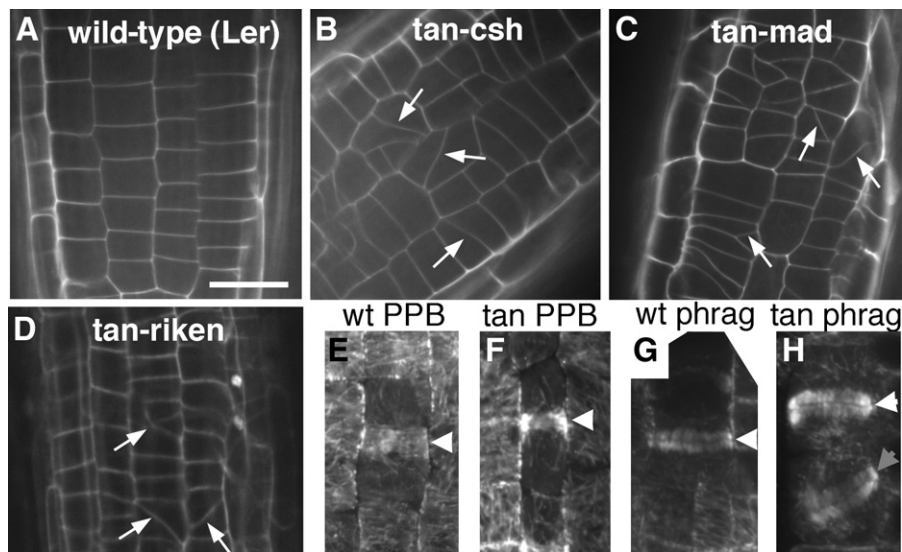
Figure 6. Genetic Analysis of *AtTAN* Function

(A–D) Root tip of 5–6-day-old wild-type (A), *tan-csh* homozygote (B), *tan-mad* homozygote (C), and *tan-riken* homozygote (D). Arrows indicate oblique cell walls indicative of recent, misoriented cell divisions.

(E–H) White arrowheads point to normal, transversely oriented PPBs (E and F) and phragmoplasts (G and H) observed in wild-type (E and G) and *tan-csh* mutant root tips (F and H). The gray arrowhead points to an oblique phragmoplast observed a in *tan-csh* mutant root tip (H). The scale bar represents 10 μm.

microtubule-dependent localization of AtTAN::YFP to the division plane. Thus, POK1/2 may help to tether AtTAN to cortical PPB microtubules during recruitment of AtTAN to the division site, or these kinesins may function to deliver AtTAN to the division site along other microtubules, such as those linking the nuclear surface to the PPB [26–28].

The persistence of broad AtTAN::YFP rings following depolymerization of existing PPB microtubules with oryzalin, and following spontaneous PPB disassembly later in the cell cycle in non-drug-treated cells, indicates that once AtTAN::YFP has been recruited to the division site, it is retained there in a microtubule-independent manner. Given that AtTAN lacks a predicted transmembrane domain, this finding suggests that it may be anchored at the division site through a direct or indirect binding interaction with an unknown transmembrane protein with very limited mobility at the division site. Recent work suggesting that PPB microtubules accomplish their function in marking of the division plane long before the PPB normally disassembles [29] is consistent with the view that microtubule-dependent recruitment of AtTAN to the division site is an important feature of division-plane establishment.

Interestingly, as cells make the transition from mitosis to cytokinesis, AtTAN::YFP narrows from an initially broad, diffuse ring to a sharper, denser ring that precisely marks the division plane during cytokinesis. This sharpening process strikingly resembles that observed for Mid1p's initially broad cortical ring, which forecasts the division plane in fission yeast and becomes a sharper ring at the onset of cytokinesis [30, 31]. Mid1p is an anillin-like protein that is unrelated in sequence to TANGLED and functions to recruit several other proteins that bring about the assembly and contraction of an F-actin-based cytokinetic ring. Coalescence of the Mid1p ring has been

proposed to be driven by an acto-myosin-dependent mechanism [31], but actin is unlikely to be involved in narrowing of the AtTAN ring because cortical F-actin is locally depleted at the cortical division site of plant cells. Thus, in spite of the resemblance of AtTAN to Mid1p in some respects, the function of the AtTAN ring, and the mechanism of its narrowing at the onset of cytokinesis, are most likely quite different. Sharpening of AtTAN rings may refine the definition of the division plane in preparation for cell-plate insertion, but further work will be required to establish the functional significance of ring sharpening and to identify the mechanism by which it occurs.

Together, our findings suggest that AtTAN is a component of the guidance cue that has been proposed to remain behind when the PPB is disassembled and to function during cytokinesis to direct the expanding phragmoplast to the former PPB site. How might AtTAN contribute to phragmoplast guidance? Like maize TAN [21], AtTAN is distantly related to the basic domains of vertebrate adenomatous polyposis coli (APC) proteins. Interestingly, in a variety of dividing cell types in *Drosophila*, APC homologs that are localized to specific cortical domains appear to interact with EB1 at the plus ends of astral microtubules to orient the mitotic spindle [32–34]. Spindle position then dictates the division plane by directing the site of contractile-ring assembly. Recent work has revealed the presence of EB1 at the plus ends of microtubules radiating from the phragmoplast and associated daughter nuclei to the cell cortex in dividing plant cells [27, 28]. Like APC, AtTAN might interact with microtubule plus ends via EB1 to help guide the expanding phragmoplast toward the division site. However, the EB1-binding domain of APC is not present in maize or *Arabidopsis* TAN, and no obvious similarities to this domain are found in any *Arabidopsis* proteins.

Thus, such a mechanism would require a cryptic EB1-binding domain in AtTAN, or the involvement of one or more as-yet-unidentified proteins linking AtTAN to EB1. Identification of the mechanism by which AtTAN at the division site interacts with the expanding phragmoplast during cytokinesis is an important goal for future studies.

Experimental Procedures

Primers Used
The following primers were used: ATLP, 5′-GATCCGTTACGAAAGT GAACACCTTTATC-3′; ATRP, 5′-ATCTCTTAGGAACCAAAACCGGA CGCTGT-3′; ATUP, 5′-TTGGGTTAATCTAGTGAGAA-3′; ATIP, 5′-TA GGTGAGGAAGCAGGAAAC-3′; JL202 (T-DNA border), 5′-CATTTTA TAATAACGCTGCGGACATCTAC-3′; Ds5-4, 5′-TACGATAACGGTC GGTACGG-3′; Ds3-4, 5′-CCGTCCCGCAAGTTAAATATG-3′; ATN-6, 5′-GCTTTGGTGAAACCCTGTTGG3′; ATN-7, 5′-GCCAAGTTACTGC CATTTCTCG-3′; ATN-20, 5′-CGAGCTCGGTAGAGTTGAACCAGAT GCTCCAG-3′; ATATG, 5′-ATGGTTGCAAGAACCCCACAG-3′; PITA, 5′-GAAGTTTCCTGCTTCCTCACC-3′; NUBQ5, 5′-GGTGCTAAGAAG AGGAAGAAT-3′; and CUBQ5, 5′-CTCCTTCTTTCTGGTAAACGT-3′.

Growth Conditions
For localization studies and examination of Arabidopsis tan mutant phenotypes at seedling stages, seedlings were grown on plates containing 1× Murashige and Skoog basal medium (MP Biomedical), 0.05% MES and 1% agarose or agar. For growth to reproductive maturity, plants were grown on soil. Plates and pots were incubated at 20°C–22°C on a 16-hr-light/8-hr-dark cycle.

Construction of Full-Length AtTAN cDNA Clone
The entire Arabidopsis TAN coding region was amplified from genomic DNA with ATLP and ATRP and used to probe 10^6 plaques from a flower-bud cDNA library (Ler background; a gift from Detlef Weigel, Max Planck Institute, Tübingen). A 1.2 kb cDNA was isolated, which was not full length. Arabidopsis flower-bud RNA was used to amplify, via RT-PCR with primers ATUP and ATIP, a 500 base fragment from the 5′ end of AtTAN, and this fragment was ligated into the cDNA clone via an internal BsaMI site to create a full-length AtTAN cDNA.

Creation of AtTAN::YFP and Maize TAN::GFP Transgenic Plants
To express a C-terminal AtTAN::YFP fusion protein from the CaMV 35S promoter, we cloned the full-length AtTAN cDNA (above) minus the stop codon in frame with YFP in the vector pEZRK-LNY, which confers kanamycin resistance in plants (http://deepgreen.stanford.edu/cell%20imaging%20site%20html/vectors.html). To express a C-terminal maize TAN::GFP fusion protein from the CaMV 35S promoter, the full-length maize TAN cDNA [21] minus the stop codon was cloned in frame with GFP in the vector pEZT-CL, which confers BASTA resistance in plants (http://deepgreen.stanford.edu/cell%20imaging%20site%20html/vectors.html). To express AtTAN::YFP from its native promoter, we used primers ATN-7 and ATN-20 to amplify a genomic fragment comprising 1.3 kb of sequence upstream of the start codon together with most of the AtTAN coding region (including all three introns). The CaMV 35S promoter and most of the AtTAN cDNA were removed from the pEZRK-based AtTAN::YFP construct (above) on a SacI/Bsu361 fragment and replaced with a SacI/Bsu361 fragment from the AtTAN genomic PCR product. After sequencing to ensure there were no errors in the coding regions of these constructs was performed, they were transformed into Arabidopsis via Agrobacterium-mediated transformation as described previously [35]. YFP or GFP rings were observed via confocal microscopy in several T2 lines for all three constructs. One of the lines expressing CaMV 35S::AtTAN::YFP was transformed with a CaMV 35S-driven CFP::α-tubulin (CFP::TUA1) construct conferring BASTA resistance [22] to generate plants coexpressing AtTAN::YFP and CFP::TUA1.

Localization of AtTAN::YFP and CFP::TUA1
AtTAN::YFP and CFP::TUA1 were examined in root tips of 4–5-day-old seedlings mounted on glass coverslips in 1× MS liquid media or water via a spinning-disk confocal-microscope system described

previously [22]. YFP was excited with 488 or 514 nm and was viewed with a 525/50 or a 570/65 nm bandpass emission filter, respectively. CFP was visualized with 442 nm excitation and a 480/40 bandpass emission filter. Image integration times varied from 400 to 800 ms with a Roper Cascade 512b camera using on-chip gain and reading off at 5 Mhz. Z series were captured with a 63× 1.2 NA water-immersion objective at 0.5 mm intervals. Two-dimensional projections and three-dimensional reconstructions of Z stacks were produced with either MetaMorph v.5.0r7 (Universal Imaging) or ImageJ v.1.34s (http://rsb.info.nih.gov/ij/). Further image processing and red-green color merges were carried out with NIH ImageJ v.1.34s or Adobe Photoshop v.8.0 (Adobe Systems). Only linear adjustments to pixel values were applied. For brightest-point projections at angles other than zero, linear interpolation was used between Z planes.

Oryzalin Treatments
Seedlings 4–5 days old and expressing AtTAN::YFP and CFP::TUA1 were treated with oryzalin in two different ways. For short-term treatments, seedlings were mounted in water and imaged as described above to identify cells with microtubule PPBs and AtTAN::YFP rings. Water was then exchanged with 5 μM oryzalin, and cells that had PPBs prior to oryzalin treatment were reanalyzed for YFP and CFP fluorescence at 5 min intervals for 10–20 min. For long-term treatments, seedlings were mounted on coverslips coated with 1× MS, 1% agar, and 0.025% methanol with or without 5 μM oryzalin. Root tips were imaged immediately for YFP and CFP fluorescence as described above. After 2 hr incubation in a humidified box inside a growth chamber, root tips were imaged again for YFP and CFP fluorescence. Images were analyzed to identify all AtTAN::YFP rings present before and after treatment. To analyze mitotic activity at the end of the treatment period, we fixed seedlings in 3:1 methanol:acetic acid and stained them for nucleic acids with 1 μM 4′-6-diamidino-2-phenylindole (DAPI) or 10 μg/ml propidium iodide (PI). PI was imaged on the spinning-disk confocal-microscope system described earlier with 488 nm excitation and a 570–650 nm bandpass emission filter. DAPI was visualized on a Nikon microscope equipped for epifluorescence imaging with a standard DAPI filter cube and a SPOT RT camera (Diagnostics) for image acquisition. Images were analyzed to identify cells with condensed chromosomes.

Generation of ton2 and pok1;2 Mutants Expressing AtTAN::YFP and CFP::TUA1
Plants expressing 35S-AtTAN::YFP and CFP::TUA1 were crossed to ton2-13/+ plants [24] (a gift from Martine Pastuglia, Centre de Versailles) and to both pok1-2;2-2 and pok1-1;2-1 double mutants [25]. In wild-type siblings of ton2 mutant or pok1;2 double-mutant F_2 progeny, diffuse cytoplasmic YFP fluorescence in interphase cells correlated reliably with the presence of YFP rings in mitotic cells. Thus, diffuse cytoplasmic YFP fluorescence allowed us to positively identify ton2 and pok1;2 mutant individuals expressing AtTAN::YFP even though AtTAN::YFP rings were faint or absent in these plants. YFP+ shoot tissue (ton2 and wild-type siblings) or root tips (pok1;2 and wild-type siblings) were scanned for cells with CFP::TUA1-labeled phragmoplasts (all genotypes), spindles (all genotypes), and PPBs (pok1;2 double mutants and wild-type siblings only). Cells with these microtubule arrays were then analyzed for localization of AtTAN::YFP.

Identification and Analysis of tan Insertion Mutants
The tan-mad allele (Ws background) was identified in collaboration with the Arabidopsis Knockout Facility at the University of Wisconsin via a PCR-based approach [36]. PCR genotyping was carried out with primers JL202 and ATRP to amplify the tan-mad mutant allele and ATRP and ATLP to amplify the wild-type allele. A BLAST search of the Cold Spring Harbor Arabidopsis Genetrap [37] database at http://genetrap.cshl.org led to identification of tan-csh (stock CSHL_GT6634; Ler background). PCR genotyping was carried out either with Ds5-4 and ATRP or with ATIP to amplify the tan-csh mutant allele and ATLP and ATRP to amplify the wild-type allele. A keyword search on At3g05330 of the RIKEN insertion database [38, 39] at http://rarge.gsc.riken.jp/dsmutant/keyword.pl resulted in identification of the tan-riken allele (line 13-0229-1, Nossen background). PCR genotyping was carried out with ATN-7 and Ds3-4 to amplify the tan-riken mutant allele and ATLP and ATRP to

amplify the wild-type allele. For all three alleles, progeny of multiple homozygous mutants, their homozygous wild-type siblings, and wild-type plants of the same genetic background were examined. Root tips from 4–6-day-old seedlings and unexpanded hypocotyls and petioles from 3-day-old seedlings were stained with 10 μg/ml propidium iodide to fluorescently label cell walls and were imaged via confocal microscopy as previously described [40]. Unexpanded pedicels were examined by scanning-electron microscopy as previously described [40]. Immunofluorescent labeling and confocal-microscopy analysis of root-tip microtubules were carried out as described previously [25].

Northern Blots and RT-PCR

RNA was extracted with TRIzol reagent (Invitrogen). For northern blots, poly A$^+$ mRNA was enriched with the PolyATract mRNA isolation kit (Promega). Northern blots were performed as described previously [41] with the full-length *AtTAN* cDNA (described earlier) as a probe. Blots were stripped and reprobed with a β-tubulin fragment [42] (a gift from Martin Yanofsky, UCSD) to demonstrate equal loading. For RT-PCR, reverse-transcriptase reactions were performed with the RETROscript kit (Ambion). PCR amplification of *AtTAN* cDNA was then carried out with primers ATATG or ATUP and ATN-6 or for reactions spanning the insertions in *tan-csh*, *tan-riken*, and *tan-mad* and ATN-6 and PITA for reactions 3′ of these insertions. As a control, a fragment of the *UBIQUITIN5* gene was amplified with primers NUBQ5 and CUBQ5.

GUS Staining

GUS activity was visualized in plants containing the *tan-csh* allele by staining with 125 μg/ml X-Gluc as described previously [43], except that tissue was incubated for 3–5 days at 37°C.

Supplemental Data

Supplemental analysis and four figures are available at http://www.current-biology.com/cgi/content/full/17/21/1827/DC1/.

References

1. Mineyuki, Y. (1999). The preprophase band of microtubules: its function as a cytokinetic apparatus in higher plants. Int. Rev. Cytol. *187*, 1–49.
2. Dixit, R., and Cyr, R.J. (2002). Spatio-temporal relationship between nuclear envelope breakdown and preprophase band disappearance in cultured tobacco cells. Protoplasma *219*, 116–121.
3. Staehelin, L.A., and Hepler, P.K. (1996). Cytokinesis in higher plants. Cell *84*, 821–824.
4. Jürgens, G. (2005). Cytokinesis in higher plants. Annu. Rev. Plant Biol. *56*, 281–283.
5. Smith, L.G. (2001). Plant cell division: Building walls in the right places. Nat. Rev. Mol. Cell Biol. *10*, 33–39.
6. Traas, J., Bellini, C., Nacry, P., Kronenberger, J., Bouchez, D., and Caboche, M. (1995). Normal differentiation patterns in plants lacking microtubular preprophase bands. Nature *375*, 676–677.
7. Vanstraelen, M., Van Damme, D., De Rycke, R., Mylle, E., Inze, D., and Geelen, D. (2006). Cell cycle-dependent targeting of a kinesin at the plasma membrane demarcates the division site in plant cells. Curr. Biol. *16*, 308–314.
8. Gunning, B.E.S. (1982). The cytokinetic apparatus: Its development and spatial regulation. In The Cytoskeleton in Plant Growth and Development, C.W. Lloyd, ed. (London: Academic Press), pp. 229–292.
9. Ota, T. (1961). The role of cytoplasm in cytokinesis of plant cells. Cytologia (Tokyo) *26*, 428–447.
10. Gunning, B.S., and Wick, S.M. (1985). Preprophase bands, phragmoplasts, and spatial control of cytokinesis. J. Cell Sci. *2*, S157–S179.
11. Palevitz, B.A. (1986). Division plane determination in guard mother cells of *Allium*: Video time-lapse analysis of nuclear movements and phragmoplast rotation in the cortex. Dev. Biol. *117*, 644–654.
12. Cleary, A.L., and Smith, L.G. (1998). The *tangled1* gene is required for spatial control of cytoskeletal arrays associated with cell division during maize leaf development. Plant Cell *10*, 1875–1888.
13. Pickett-Heaps, J.D., and Northcote, D.H. (1966). Organization of microtubules and endoplasmic reticulum during mitosis and cytokinesis in wheat meristems. J. Cell Sci. *1*, 109–120.
14. Cleary, A.L., Gunning, B.E.S., Wasteneys, G.O., and Hepler, P.K. (1992). Microtubule and F-actin dynamics at the division site in living *Tradescantia* stamen hair cells. J. Cell Sci. *103*, 977–988.
15. Liu, B., and Palevitz, B.A. (1992). Organization of cortical microfilaments in dividing root cells. Cell Motil. Cytoskeleton *23*, 252–264.
16. Hoshino, H., Yoneda, A., Kumagai, F., and Hasezawa, S. (2003). Roles of actin-depleted zone and preprophase band in determining the division site of higher-plant cells, a tobacco BY-2 cell line expressing GFP-tubulin. Protoplasma *222*, 157–165.
17. Buschmann, H., Chan, J., Sanchez-Pulido, L., Andrade-Navarro, M.A., Doonan, J.H., and Lloyd, C.W. (2006). Microtubule-associated AIR9 recognizes the cortical division site at preprophase and cell-plate insertion. Curr. Biol. *16*, 1938–1943.
18. Hall, Q., and Cannon, M.C. (2002). The cell wall hydroxyproline-rich glycoprotein RSH is essential for normal embryo development in *Arabidopsis*. Plant Cell *14*, 1161–1172.
19. Van Damme, D., Coutuer, S., De Rycke, R., Bouget, F.Y., Inzé, D., and Geelen, D. (2006). Somatic cytokinesis and pollen maturation in *Arabidopsis* depend on TPLATE, which has domains similar to coat proteins. Plant Cell *18*, 3502–3518.
20. Smith, L.G., Hake, S.C., and Sylvester, A.W. (1996). The *tangled1* mutation alters cell division orientations throughout maize leaf development without altering leaf shape. Development *122*, 481–489.
21. Smith, L.G., Gerttula, S.M., Han, S., and Levy, J. (2001). TANGLED1: A microtubule binding protein required for the spatial control of cytokinesis in maize. J. Cell Biol. *152*, 231–236.
22. Paredez, A.R., Somerville, C.R., and Ehrhardt, D.W. (2006). Visualization of cellulose synthase demonstrates functional association with microtubules. Science *312*, 1491–1495.
23. Samuels, A.L., Giddings, T.H., Jr., and Staehelin, L.A. (1995). Cytokinesis in tobacco BY-2 and root tip cells: A new model of cell plate formation in higher plants. J. Cell Biol. *130*, 1345–1357.
24. Camilleri, C., Azimzadeh, J., Pastuglia, M., Bellini, C., Granjean, O., and Bouchez, D. (2002). The *Arabidopsis* TONNEAU2 gene encodes a putative novel protein phosphatase 2A regulatory subunit essential for the control of the cortical cytoskeleton. Plant Cell *14*, 833–845.
25. Müller, S., Han, S., and Smith, L.G. (2006). Two kinesins are involved in the spatial control of cytokinesis in *Arabidopsis*. Curr. Biol. *16*, 888–894.
26. Wick, S.M. (1985). Immunofluorescence microscopy of tubulin and microtubule arrays in plant cells. III. Transition between mitotic/cytokinetic and interphase microtubule arrays. Cell Biol. Int. Rep. *9*, 357–371.
27. Dhonukshe, P., Mathur, J., Hulskamp, M., and Gadella, T.W.J. (2005). Microtubule plus-ends reveal essential links between intracellular polarization and localized modulation of endocytosis during division-plane establishment in plant cells. BMC Biol. *3*, 11.

28. Chan, J., Calder, G., Fox, S., and Lloyd, C. (2005). Localization of the microtubule end binding protein EB1 reveals alternative pathways of spindle development in *Arabidopsis* suspension cells. Plant Cell *17*, 1737–1748.

29. Marcus, A.I., Dixit, R., and Cyr, R.J. (2005). Narrowing of the pre-prophase microtubule band is not required for cell division plane determination in cultured plant cells. Protoplasma *226*, 169–174.

30. Wu, J.-Q., Kuhn, J.R., Kovar, D.R., and Pollard, T.D. (2003). Spatial and temporal pathway for assembly and constriction of the contractile ring in fission yeast cytokinesis. Dev. Cell *5*, 723–734.

31. Wu, J.-Q., Sirotkin, V., Kovar, D.R., Lord, M., Beltzner, C.C., Kuhn, J.R., and Pollard, T.D. (2006). Assembly of the cytokinetic contractile ring from a broad band of nodes in fission yeast. J. Cell Biol. *174*, 391–402.

32. Lu, B., Roegiers, F., Jan, L.Y., and Jan, Y.N. (2001). Adherens junctions inhibit asymmetric division in the *Drosophila* epithelium. Nature *409*, 522–525.

33. McCartney, B.M., McEwen, D.G., Grevengoed, E., Maddox, P., Bejsovec, A., and Peifer, M. (2001). *Drosophila* APC2 and Armadillo participate in tethering mitotic spindles to cortical actin. Nat. Cell Biol. *3*, 933–938.

34. Yamashita, Y.M., Jones, D.L., and Fuller, M.T. (2003). Orientation of asymmetric stem cell division by the APC tumor suppressor and centrosome. Science *301*, 1547–1550.

35. Clough, S.J., and Bent, A.F. (1998). Floral dip: A simplified method for *Agrobacterium*-mediated transformation of *Arabidopsis thaliana*. Plant J. *16*, 735–743.

36. Krysan, P.J., Young, J.C., and Sussman, M.R. (1999). T-DNA as an insertional mutagen in *Arabidopsis*. Plant Cell *11*, 2283–2290.

37. Martienssen, R.A. (1998). Functional genomics: probing plant gene function and expression with transposons. Proc. Natl. Acad. Sci. USA *95*, 2021–2026.

38. Ito, T., Motohashi, R., Kuromori, T., Mizukado, S., Sakurai, T., Kanahara, H., Seki, M., and Shinozaki, K. (2002). A new resource of locally transposed *Dissociation* elements for screening gene-knockout lines in silico on the *Arabidopsis* genome. Plant Physiol. *129*, 1695–1699.

39. Kuromori, T., Hirayama, T., Kiyosue, Y., Takabe, H., Mizukado, S., Sakurai, T., Akiyama, K., Kamiya, A., Ito, T., and Shinozaki, K. (2004). A collection of 11 800 single-copy *Ds* transposon insertion lines in *Arabidopsis*. Plant J. *37*, 897–905.

40. Djakovic, S.N., Dyachok, J., Burke, M.P., Frank, M.J., and Smith, L.G. (2006). BRICK1/HSPC300 acts with SCAR and the ARP2/3 complex to regulate epidermal cell shape in *Arabidopsis*. Development *133*, 1091–1100.

41. Luehrsen, K.B. (1994). Northern blotting. In The Maize Handbook, V. Walbot and M. Freeling, eds. (New York: Springer-Verlag), pp. 572–574.

42. Marks, M.D., West, J., and Weeks, D.P. (1987). The relatively large beta-tubulin gene family of *Arabidopsis* contains a member with an unusual transcribed 5′ non-coding sequence. Plant Mol. Biol. *10*, 91–104.

43. Meister, R.J., Kotow, L.M., and Gasser, C.S. (2002). SUPERMAN attenuates positive INNER NO OUTER autoregulation to maintain polar development of *Arabidopsis* ovule outer integuments. Development *129*, 4281–4289.

Accession Numbers

The GenBank accession number for the Arabidopsis TANGLED sequence reported in this paper is DQ631804.